

Geophysical Research Letters

RESEARCH LETTER

10.1029/2019GL082931

Key Points:

- Utilization of satellite-derived surface salinity to study freshwater fluxes and salinity variability in the Gulf of Mexico is presented
- Loop Current System configuration, not river discharge, determines patterns of lateral freshwater fluxes and surface salinity signatures
- Loop Current System configurations are classified as favorable or not for strong freshwater flux during summer months

Correspondence to:

R. J. Brokaw,
rbrokaw@email.sc.edu

Citation:

Brokaw, R. J., Subrahmanyam, B., & Morey, S. L. (2019). Loop current and eddy-driven salinity variability in the Gulf of Mexico. *Geophysical Research Letters*, 46, 5978–5986. <https://doi.org/10.1029/2019GL082931>

Received 20 MAR 2019

Accepted 12 MAY 2019

Accepted article online 2 JUN 2019

Published online 7 JUN 2019

Loop Current and Eddy-Driven Salinity Variability in the Gulf of Mexico

Richard J. Brokaw¹ , Bulusu Subrahmanyam¹ , and Steven L. Morey² 

¹School of the Earth, Ocean, and Environment, University of South Carolina, Columbia, SC, USA, ²School of the Environment, Florida A&M University, Tallahassee, FL, USA

Abstract The Loop Current System, involving the Loop Current and Loop Current Eddies, is the principal circulation feature in the Gulf of Mexico, which exhibits salinity gradients due to Mississippi River system freshwater discharge and large salinity variability on seasonal timescales. This research uses satellite-derived sea surface salinity from NASA's Soil Moisture Active Passive and ESA's Soil Moisture and Ocean Salinity missions with altimetric sea surface height data to observe and quantify the redistribution of low-salinity water by Loop Current System interaction. Freshwater flux in this region during summer months is modulated by Loop Current System configuration as classified by three states. An extended Loop Current transports low-salinity water southward to the Florida Straits. A Loop Current eddy near the Louisiana-Texas shelf recirculates low-salinity water within the central Gulf. During a retracted Loop Current, no interaction occurs and low-salinity water remains close to the coast in the northern Gulf.

Plain Language Summary The Gulf of Mexico receives freshwater from the Mississippi and Atchafalaya Rivers with an annual peak during spring due to snow melt over the upper part of the watershed. The fresh water forms a low-salinity water plume, which evolves based on local wind forcing as well as circulation features associated with the Loop Current System. The Loop Current brings Caribbean Sea water northward into the Gulf of Mexico and transports waters out of the Gulf through the Florida Straits where it feeds into the Gulf Stream. While inside the Gulf, the Loop Current can extend northward to the Mississippi-Alabama coast. When extended northward, the Loop Current advects low-salinity water eastward along the Mississippi/Alabama/Florida shelf, and southward along the West Florida Shelf. This low-salinity water then exits the Gulf through the Florida Straits. Additionally, the Loop Current occasionally sheds anticyclonic eddies which migrate westward to the Texas coast, and can recirculate low-salinity water in the central Gulf of Mexico. Analysis of nearly a decade of satellite salinity data shows a preference for events of freshwater flux toward the southeastern Gulf of Mexico during the late summer months with substantial interannual variability linked with the configuration of the Loop Current System.

1. Introduction

The Gulf of Mexico (GoM) is a semienclosed sea with circulation dominated by a branch of the North Atlantic's western boundary current system (the Loop Current System—LCS) flowing through the basin and receiving freshwater from one of the largest river systems in the world. Marked seasonal increases in Mississippi and Atchafalaya Rivers discharge contribute freshwater to the northern Gulf during spring (Bratkovich et al., 1994). Freshwater input forms a low-salinity water (LSW) plume that interacts with the LCS. The LCS is composed of the Loop Current (LC), which sheds anticyclonic Loop Current Eddies (LCEs) on time scales of approximately 3 to 17 months (Sturges & Leben, 2000). This energetic LC feeds into the Gulf Stream through the Florida Straits. The GoM is also environmentally and economically important to the United States, Mexico, and Cuba. The LCS redistributes biota and nutrients essential for GoM ecosystems. Elevated nutrient and pigment concentrations are associated with low salinity water as rivers supply both fresh water and nutrients to the Gulf (Hiester et al., 2017; Zavala-Hidalgo et al., 2014). The upper ocean stratification within the GoM affects the intensification of tropical cyclones through the fluxes of heat energy to the atmosphere from the deep mixed layer associated with the LCS (Gierach & Subrahmanyam, 2006).

The LC transitions slowly from a retracted position flowing from the Yucatan Channel to the Florida Straits, to an extended one, which reaches toward the Mississippi-Alabama-Florida (MAFLA) Shelf. This extended

state leads to the shedding of a large anticyclonic LCE, after which the LC returns abruptly to its retracted state (Alvera-Azcárate et al., 2008). GoM dynamics are dominated by a combination of “frontal” cyclonic eddies that occasionally pinch the LC (Le Hénaff et al., 2012) and the mesoscale eddy field associated with the LCS. In contrast to the strong seasonality in freshwater input to the GoM, the intrusion of the LC and positions of LCEs within the GoM have no strong seasonal cycle causing the interactions of LSW with the LCS to differ greatly from year to year.

Some studies (Morey, Martin, et al., 2003; Morey, Schroeder, et al., 2003; Otis et al., 2019; Schiller et al., 2011; Schiller & Kourafalou, 2014) have investigated transport of LSW away from the northern GoM and have expanded the understanding of the pathways of this LSW and seasonality. Additionally, previous episodes of long-distance transport of Mississippi waters have been documented first in 1993 (Gilbert et al., 1996; Ortner et al., 1995), in 2004 (Hu et al., 2005), and in 2014 (Le Hénaff & Kourafalou, 2016). However, these studies have focused on singular events, and there has been no research to our knowledge into the varying spatial patterns of the GoM surface salinity field. The motivation for this research is to investigate the connection between the LCS and seasonal and interannual changes in GoM surface salinity field and lateral freshwater fluxes. We aim to characterize the LCS configurations that lead to the different spatial distributions of LSW throughout the Gulf. Specifically, we investigate the role of the extended LC and LCEs in determining patterns of lateral freshwater fluxes, and hence surface salinity signatures in the GoM. Differing patterns of surface salinity signatures are important in understanding the fate of the freshwater from the Mississippi and Atchafalaya rivers, which has potential biological impacts in areas such as the Florida Straits and can alter the upper ocean stratification of the central GoM.

Through the use of satellite-derived sea surface salinity (SSS) and altimetric sea level anomaly (SLA), we can observe how the LC interacts with the seasonally present LSW in the northern GoM. From these data, we can observe the surface salinity signatures associated with freshwater input. Evaluating together the measures of salinity, river discharge, and merged altimetry products to observe geostrophic velocities in the GoM helps provide a comprehensive view of the LCS interaction with LSW plumes contributed by the Mississippi and Atchafalaya Rivers.

2. Data and Methods

The NASA's Soil Moisture Active Passive (SMAP) SSS level 3 V4.0 daily product is derived using an 8-day running mean (consistent with complete global coverage of SMAP's orbit) and is produced by the NASA Jet Propulsion Laboratory (JPL, openly available at https://podaac.jpl.nasa.gov/dataset/SMAP_JPL_L3_SSS_CAP_8DAY-RUNNINGMEAN_V42?ids=&values=&search=SMAP,doi:10.5067/SMP42-3TPCS) from 2 April 2015 to present with 0.25° resolution. The Combined Active-Passive retrieval algorithm initially developed by JPL for Aquarius/SAC-D is extended to this SMAP product. The ESA's Soil Moisture and Ocean Salinity (SMOS) SSS product used is the LOCEAN level 3 V3 9-day composite maps produced by LOCEAN/ACRI-ST, obtained from the Centre Aval de Traitement des Données SMOS from 4 January 2010 to present at 25-km resolution. This debiased version 3 product improves upon the previous version 2 product with better adjustment for land-sea bias close to the coast and high latitudinal biases (Boutin, Vergely, & Khvorostyanov, 2018; Boutin, Vergely, Marchand, et al., 2018). The monthly averages of both SMAP and SMOS SSS data sets were computed for this study. Vazquez-Cuervo et al. (2018) compared the JPL SMAP and LOCEAN SMOS SSS with other satellite-derived SSS products, buoy-derived, and World Ocean Database (WOD) in situ data in the GoM, and found that these data sets consistently reproduce seasonal and spatial variability in SSS associated with river discharge. This comparison also found that the seasonal “spring freshening” near the coast is best represented in the JPL SMAP and LOCEAN SMOS products.

Geostrophic currents used to examine surface currents, and eddies are derived from the AVISO multimission merged daily altimetry product. Data from multisatellite altimeter missions are processed to provide mapped SLA fields with respect to a 20-year mean. This data set is provided by the Copernicus Marine Environment Monitoring Service, (marine.copernicus.eu) at daily 0.25° resolution. Geostrophic velocities computed from the sea level data are used in combination with SSS anomalies to compute the surface advective freshwater fluxes computed as:

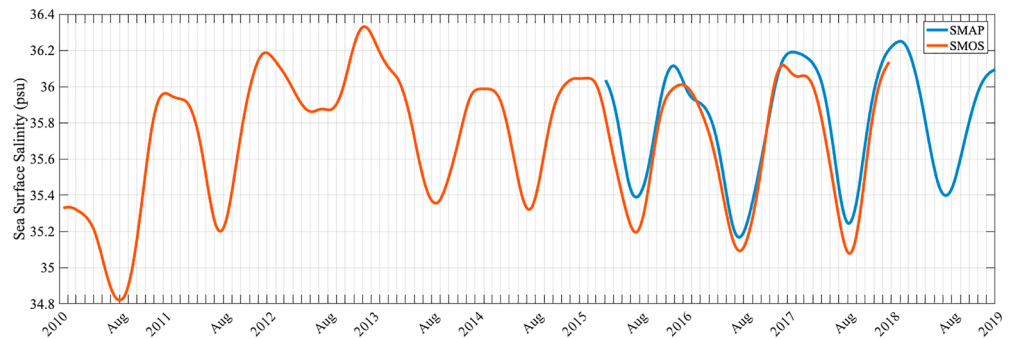


Figure 1. European Space Agency's SMOS (2010–2017) and National Aeronautics and Space Administration's SMAP (2015–2018) sea surface salinity averaged over the GoM. SMOS = Soil Moisture and Ocean Salinity; SMAP = Soil Moisture Active Passive.

$$\text{Zonal} : F = U \times Sfw \times dx \quad (1)$$

$$\text{Meridional} : F = V \times Sfw \times dx \quad (2)$$

This calculation follows the approach of Münchow et al. (2006), where $U(V)$ is the eastward (northward) velocity (m/s), Sfw is the freshwater salinity anomaly computed in equation (3), and dx is the width (m) of the segment across which flux is calculated. The computation of Sfw follows the approach of Mazloff et al. (2010):

$$Sfw = (Sref - SSS) / Sref \quad (3)$$

where $Sref$ is the reference salinity (36.5 here for the GoM), and SSS is the sea surface salinity at a point, provided here by SMOS and SMAP SSS data. Boxed averages of these fluxes were taken for: MAFLA Shelf (28.5–30°N, 89–86°W), Florida Straits (23.5–24.75°N, 83.5–80°W), West Florida Shelf (23.5–29°N, 86–83°W), and Yucatan Channel (21–23°N, 86.5–85°W).

Daily river discharge of the Mississippi River at the Baton Rouge, LA (USGS 07374000) and Atchafalaya River at Morgan City, LA (USGS 07381600) gauging stations were obtained from the United States Geological Survey National Water Information System (USGS, <https://waterdata.usgs.gov/nwis>). Analysis of river discharge in conjunction with the other described products provides a more complete view of the factors that could lead to seasonal and interannual changes of GoM surface salinity.

3. Results

A strong seasonal cycle of SSS in the GoM is evident in the time series of basin-averaged SSS (Figure 1). SSS maxima occur in the winter months of January and February every year, while SSS minima occur in the late summer months of July and August every year. Morey et al. (2003) showed a similar seasonal pattern in surface salinity along the eastern side of the typical LC position using a numerical model forced by climatology wind, heat, and freshwater fluxes. Since we aim to investigate the interaction of this seasonally present LSW and the LCS, we focus on the month of August which exhibits the lowest SSS values and therefore the greatest amount of LSW at the surface.

Varying spatial patterns of surface salinity throughout the GoM are shown in Figure 2. LSW is dominantly found in the northern and northeastern GoM, with SSS values reaching lower than 33, while the southwestern GoM is dominated by high SSS values reaching higher than 37. However, the low SSS values are not always confined to the northeastern GoM and can be observed in other locations in the GoM along the West Florida Shelf, central GoM, and occasionally near the Florida Straits. The distinct interactions of the LCS with LSW produce varying patterns of surface advective freshwater flux values (Figures 3 and 4) and produce differing SSS signatures as well.

The LCS configurations are classified based on the SSS spatial patterns related to the LCS-influenced lateral freshwater fluxes. The first classification (#1) occurs when the LC extends northward to the MAFLA shelf

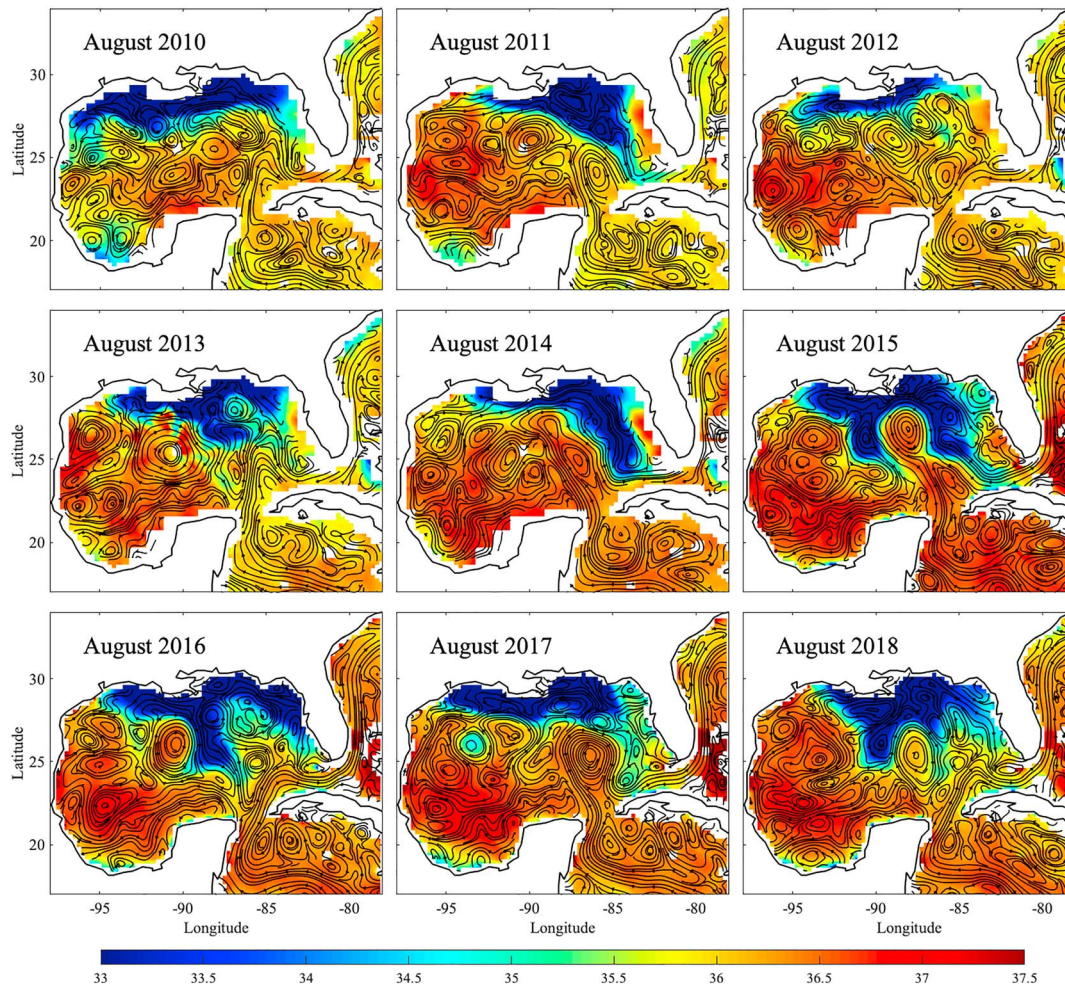


Figure 2. Monthly European Space Agency's Soil Moisture Ocean Salinity (2010–2014) and National Aeronautics and Space Administration's Soil Moisture Active Passive (2015–2018) sea surface salinity and altimetric geostrophic current streamlines for August 2010–2018.

during August of 2011, 2014, 2015, and 2017 (Figure 2). While in this configuration, LSW is advected eastward along the MAFLA shelf and southward along the West Florida Shelf by the anticyclonic rotation of the LC. Figures 3a–3d show the SSS signatures for this classification #1, which are a result of the advection of LSW away from the coast by the LC. The eastward advection of LSW is evident in the strong positive zonal freshwater fluxes reaching $800 \text{ m}^2/\text{s}$ along the MAFLA shelf (Figures 3e–3h). Southeasterly prevailing winds during summer drive Ekman transport in the surface layer, resulting in eastward transport of LSW away from the Mississippi Delta toward the deeper waters of the De Soto Canyon where it can be entrained in offshore circulation features such as eddies and the LC (Morey, Schroeder, et al., 2003). As the northern extent of the LC entrains and transports this LSW eastward, its anticyclonic rotation pulls the water southward in the region of the western shelf-break of the West Florida Shelf (85°W). Southward LSW advection is evident in strong negative meridional freshwater flux (exceeding $600 \text{ m}^2/\text{s}$) near the West Florida Shelf, reaching southward to the western tip of Cuba (Figures 3i–3l). Positive values of zonal freshwater fluxes from $400\text{--}600 \text{ m}^2/\text{s}$ can be observed near the Florida Straits (Figures 3e–3h). Despite different LCS-LSW interactions, there is consistent eastward zonal freshwater flux through the Florida Straits (Figures 3 and 4), suggesting that LSW exits the GoM via the Florida Current. The varying magnitudes of this eastward flux through the Florida Straits are discussed later in this section.

The second classification (#2) occurs when there is an anticyclonic LCE present in the central/western GoM, observed during August of 2013, 2015, 2016, and 2018. In this instance, the LCE circulates LSW away from the northern GoM but does not always transport this water toward the Florida Straits. The LCE entrains and

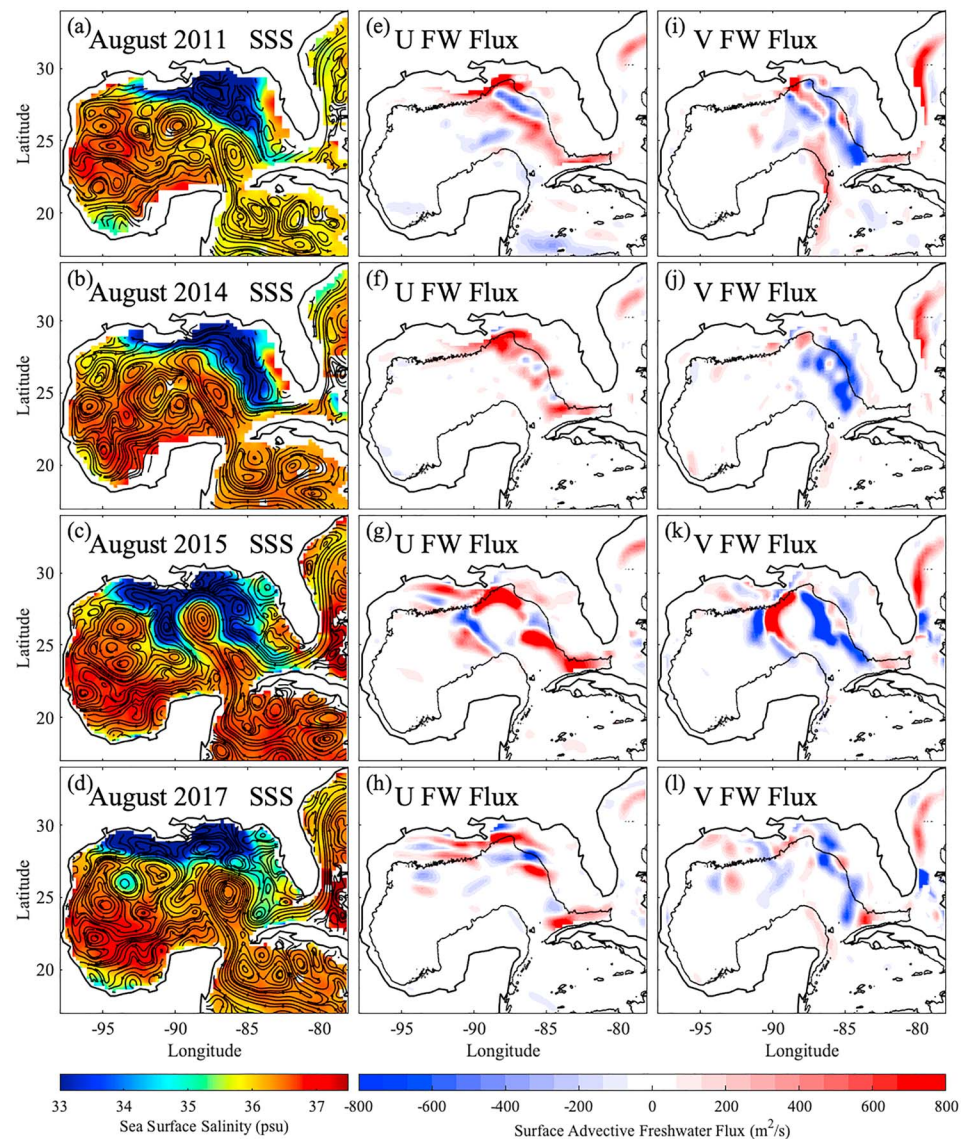


Figure 3. Monthly averaged Soil Moisture and Ocean Salinity (2011; 2014) and Soil Moisture Active Passive (2015; 2017) sea surface salinity and geostrophic current streamlines (a–d), zonal (U) advective freshwater flux (e–h); positive values represent eastward flux, and meridional (V) advective freshwater flux (i–l); positive values represent northward flux, for years described by classification #1 (August 2011, 2014, 2015, and 2017). The black lines offshore (e–l) represent the 1,000-m isobath. FW = freshwater.

transports LSW off of the MAFLA and Louisiana-Texas (**LATEX**) shelves over the deep central GoM, creating a cross-shelf transport mechanism, which is shown in the strong negative meridional freshwater fluxes reaching $800 \text{ m}^2/\text{s}$ at $90\text{--}91^\circ\text{W}$ (Figures 4i–4l). Southward meridional freshwater flux near the MAFLA and LATEX shelves (Figures 4i–4l) suggests that LSW can be entrained by the mesoscale eddy field and transported offshore in the northwestern GoM. The location of the LCE within the central GoM, which relies on the timing of its separation from the LC (Sturges et al., 1992), dictates its point of interaction with the LSW plume, which suggests that the variation in westward LCE propagation affects the patterns of lateral freshwater fluxes and surface salinity signatures.

During August of 2018, there are two LCEs present within the GoM separated by a smaller, cyclonic eddy. The first decaying LCE is located in the western GoM at 25°N , 93°W . The northeastern edge of this LCE plays a role in the southward advection of LSW, shown in the negative meridional freshwater flux south of Mississippi in Figure 4l. The second LCE located at 25°N , 88°W has a similar effect on the LSW as an

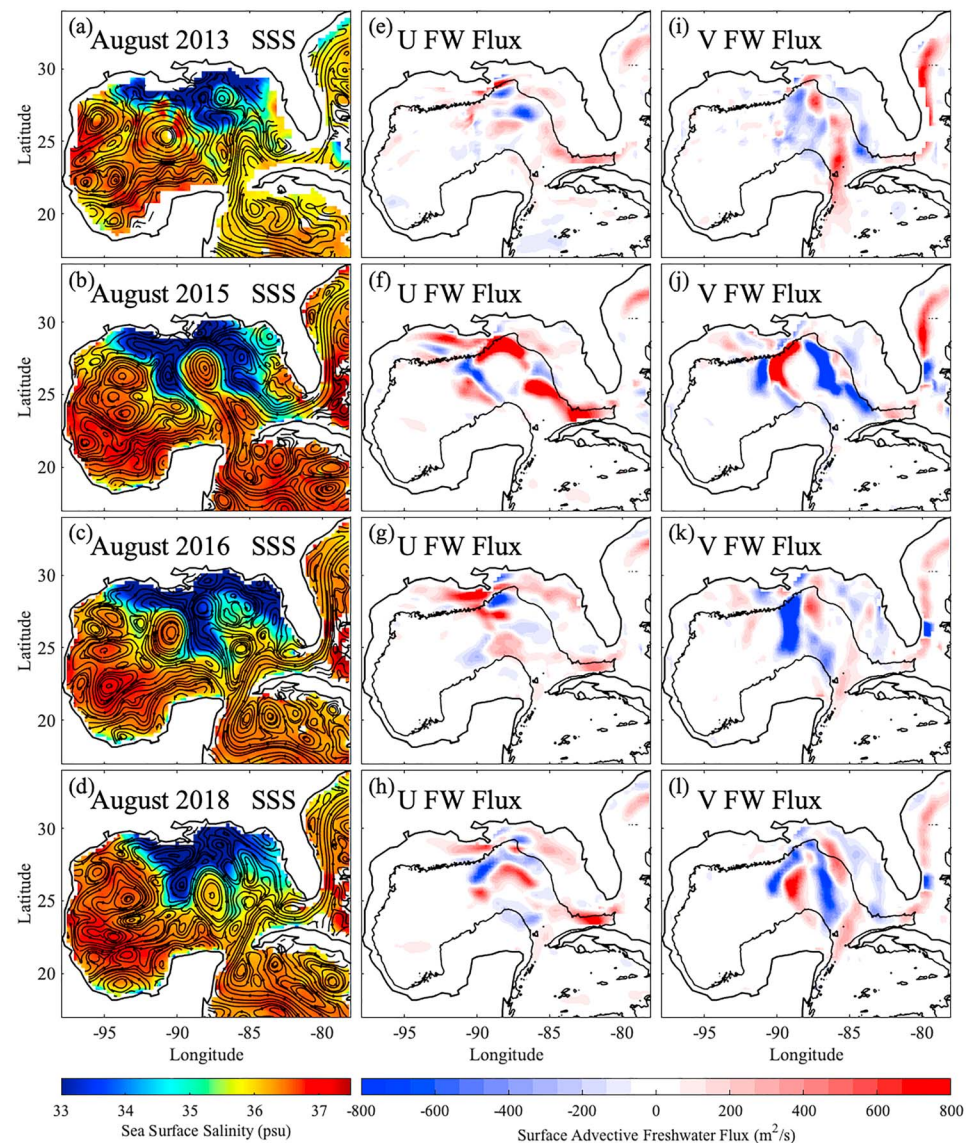


Figure 4. Same as Figure 3, for years which fit classification #2 (Soil Moisture and Ocean Salinity 2013; Soil Moisture Active Passive 2015, 2016, 2018). SSS = sea surface salinity; FW = freshwater.

extended LC, with eastward zonal (Figure 4h) and southward meridional freshwater flux (Figure 4l). An interesting aspect of this LCS-LSW interaction is a dipole created by this newer LCE and the small anticyclonic eddy. This dipole results in northward advection of LSW toward the northeastern GoM indicated by positive meridional freshwater flux (Figure 4l). The same northward advection of LSW occurs in August 2015 (Figure 4j). This is similar to the August 2013 event, where an LCE located south of the LATEX shelf transports LSW toward the central GoM, without connection to the LC. In August 2016, the LCE located at 26°N, 91°W has a different effect on the distribution of the LSW. The northern edge of this LCE entrains LSW from the LATEX shelf. This, in conjunction with the cyclonic eddy at 27°N, 88°W, creates a dipole resulting in very strong southward LSW advection as evident in the negative meridional freshwater fluxes at 89°W (Figure 4k). The resultant SSS signature is a band of low-salinity waters extending into the southern central GoM toward the Yucatan Peninsula (Figure 4c). Additionally, westward movement of LSW occurs during August of both 2016 and 2018, shown by negative zonal freshwater fluxes reaching 300 m²/s near the Campeche Bank (Figures 4g and 4h). The LCS can display features pertaining to both classifications #1 and #2, as was the case during August 2015 in which the LCE and extended LC create a distinct pattern. The characteristics leading to this distinct “horseshoe

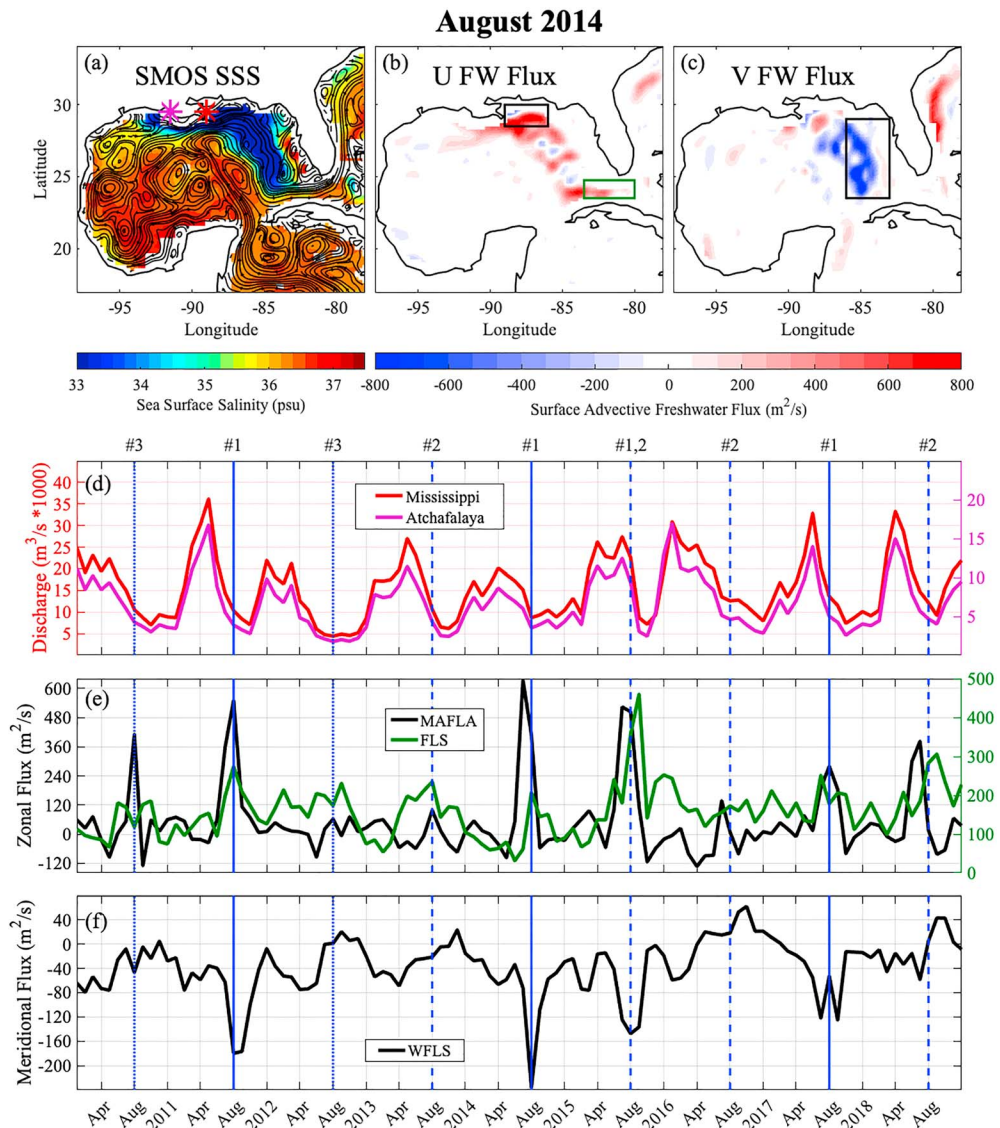


Figure 5. August 2014 maps of (a) Soil Moisture and Ocean Salinity (SMOS) sea surface salinity (SSS) and geostrophic current streamlines, (b) zonal (U) advective freshwater flux, and (c) meridional (V) advective freshwater flux. (d) Mississippi (red) and Atchafalaya (purple) river discharge, river mouths indicated by stars on map (a). (e) Boxed average zonal advective freshwater flux over the Mississippi-Alabama-Florida (MAFLA) shelf and through the Florida Straits (FLS), areas indicated in (b) by black and green boxes, respectively. (f) Boxed average meridional advective freshwater flux over the West Florida Shelf (WFLS) indicated in (c) by the black box. Blue lines mark August of years that fit classifications #1 (solid), #2 (dashed), and #3 (dotted). FW = freshwater.

pattern,” such as the soil moisture and river flooding that occurred in Texas, are discussed by Fournier et al. (2016). The low-salinity bands extending over the deep central GoM evident in the SSS signatures of August 2013 (25–27°N, 88–87°W), 2015 (25–27°N, 91–90°W), 2016 (25–27°N, 89–88°W), and 2018 (25–27°N, 90–89°W) do not connect to the eastward flowing portion of the LC, and therefore do not exit the GoM through the Florida Straits.

The differing magnitudes of monthly river discharge, meridional, and zonal advective freshwater flux for each year included in this study (2010–2018) are shown in Figure 5. Years that fit classification #1 exhibit the greatest positive zonal freshwater fluxes along the MAFLA shelf (Figure 5e), with boxed average values of 550 m^2/s (2011), 633 m^2/s (2014), 523 m^2/s (2015), and 279 m^2/s (2017). The same years exhibit the greatest negative meridional freshwater fluxes along the West Florida Shelf (Figure 5f), with boxed average values

of $-180 \text{ m}^2/\text{s}$ (2011), $-236 \text{ m}^2/\text{s}$ (2014), $-148 \text{ m}^2/\text{s}$ (2015), and $-125 \text{ m}^2/\text{s}$ (2017). During the years that fit classification #1, the maximum eastward flux through the Florida Straits occurs simultaneously with maximum eastward flux along the MAFLA shelf (Figure 5e). However, in years that fit classification #2, the peak eastward flux through the Florida Straits occurs approximately 2–4 months after peak eastward flux along the MAFLA shelf. The circulation of LSW within the central GoM without clear connection to the Florida Straits in August of 2016 and 2018 helps explain the lag in maximum zonal flux through the Florida Straits region during these years. The year 2016 seems to be an anomalous year, where LSW is transported into the central GoM without clear connection to the LC (Figure 4b). This explains the lack of peak zonal freshwater flux through the Florida Straits during 2016 (Figure 5e). When comparing yearly differences in river discharge (Figure 5d) to the zonal and meridional freshwater fluxes (Figures 5e and 5f), there is no clear relationship between peaks in river discharge and peaks in freshwater flux. During April 2014, peak river discharge reaches a record minimum of 20,146 and 8,640 m^3/s for the Mississippi and Atchafalaya Rivers, respectively. Despite low input, both meridional and zonal freshwater fluxes reach a record maximum in 2014. August of 2014 also displays one of the clearest connections of LSW from its source to the Florida Straits (Figure 3b).

The third and final classification occurs in years where there is no notable LCS-LSW interaction, which can be observed during 2010 and 2012 (Figure 2). The river discharge values of 2010 and 2012 are not anomalously low (Figure 5d), but still there is very little zonal and meridional freshwater flux. Additionally, the SSS signatures displayed during these years show very little, if any, movement of LSW away from its source in the northern GoM (Figure 2). With no LCS-LSW interaction, strong values of zonal and meridional surface advective freshwater fluxes are not observed, and LSW remains close to its source in the northern GoM.

4. Conclusions

An extended LC in classification #1 establishes a clear pathway for the offshore transport of seasonally present LSW, which is advected eastward from the MAFLA shelf and southward along the West Florida Shelf. LSW is transported toward the Florida Straits, where it exits the GoM. Without this direct pathway, the LSW has different fates within the GoM, and hence the GoM exhibits differing patterns in SSS. As defined by classification #2, when there is an LCE present in the central GoM, it entrains and transports LSW across the MAFLA shelf, along the surface toward the southern GoM. This LSW reaches southward as narrow low-salinity bands, which do not directly connect to the retracted LC. This LCE can also transport the LSW westward, and even northward back toward its source, establishing a recirculation of LSW within the central GoM. This lack of direct connection results in advective freshwater flux through the Florida Straits that is both smaller in magnitude and lags behind advective freshwater flux in other regions of the GoM. This suggests that the LCS can in part control the net export of freshwater from the GoM to the Atlantic Ocean. During years defined as classification #3, no notable LCS-LSW interaction occurs, and the seasonally present LSW remains close to its source in the northern GoM. These years do not exhibit strong patterns of zonal or meridional surface advective freshwater fluxes, and therefore, there is minimal redistribution of LSW to other areas of the GoM. Although river discharge of the Mississippi and Atchafalaya Rivers fluctuate yearly, these varying discharge rates do not affect the spatial distribution of SSS within the GoM. This suggests that the configuration of the LCS plays the primary role in determining patterns of surface advective freshwater flux and hence SSS signatures in the GoM. The seasonal input of freshwater via river discharge forming LSW, and the lateral advection of this LSW away from the northern GoM by the LCS causes a decrease in overall SSS of the GoM. This helps establish the seasonal cycle of SSS with yearly minima occurring in late summer and maxima occurring in winter.

References

- Alvera-Azcárate, A., Barth, A., & Weisberg, R. H. (2008). The surface circulation of the Caribbean Sea and the Gulf of Mexico as inferred from satellite altimetry. *Journal of Physical Oceanography*, 39(3), 640–657. <https://doi.org/10.1175/2008JPO3765.1>
- Boutin, J., Vergely, J. L., & Khvorostyanov, D. (2018). SMOS SSS L3 maps generated by CATDS CEC LOCEAN. debias V3.0. SEANOE. <https://doi.org/10.17882/52804#57467>
- Boutin, J., Vergely, J. L., Marchand, S., D'Amico, F., Hasson, A., Kolodziejczyk, N., et al. (2018). New SMOS sea surface salinity with reduced systematic errors and improved variability. *Remote Sensing of Environment*, 214, 115–134. <https://doi.org/10.1016/j.rse.2018.05.022>

Acknowledgments

This work is supported by the UofSC's Magellan Scholarship awarded to R. J. B. S. L. M.'s contribution to this work is supported by the NOAA Center for Coastal and Marine Ecosystems (NOAA Office of Education Educational Partnership Program award NA16SEC4810009), and the contents are solely the responsibility of the award recipient and do not necessarily represent the official views of the U.S. Department of Commerce, NOAA. SLA are provided by the Copernicus Marine Environmental Monitoring Service (CMEMS; marine.copernicus.eu). SMAP data are available via NASA's Jet Propulsion Lab Physical Oceanography Distributed Active Archive Center, and SMOS is from Centre Aval de Traitement des Données SMOS (CATDS). River data are obtained from United States Geological Survey National Water Information System. The authors would like to thank the anonymous reviewers and Editor, whose comments significantly contributed to the improvement of this paper.

- Bratkovich, A., Dinnel, S. P., & Goolsby, D. A. (1994). Variability and prediction of freshwater and nitrate fluxes for the Louisiana-Texas Shelf: Mississippi and Atchafalaya River source functions. *Estuarine Research Federation*, 17(4), 766–778. <https://doi.org/10.2307/1352746>
- Fournier, S., Reager, J. T., Lee, T., Vazquez-Cuervo, J., David, C. H., & Gierach, M. M. (2016). SMAP observes flooding from land to sea: The Texas event of 2015. *Geophysical Research Letters*, 43, 10,338–10,346. <https://doi.org/10.1002/2016GL070821>
- Gierach, M., & Subrahmanyam, B. (2006). Satellite data analysis of the upper ocean response to Hurricanes Katrina and Rita (2005) in the Gulf of Mexico. *IEEE Geoscience and Remote Sensing Letters*, 4(1), 132–136. <https://doi.org/10.1109/LGRS.2006.887145>
- Gilbert, P. S., Lee, T. N., & Podesta, G. P. (1996). Transport of anomalous low salinity waters from the Mississippi River flood of 199 to the straits of Florida. *Continental Shelf Research*, 16(8), 1065–1085. [https://doi.org/10.1016/0278-4343\(95\)00056-9](https://doi.org/10.1016/0278-4343(95)00056-9)
- Hiestar, H. R., Morey, S. L., Dukhovskoy, D. S., Chassignet, E. P., Kourafalou, V. H., & Hu, C. (2017). A topological approach for quantitative comparisons of ocean model fields to satellite ocean color data. *Methods in Oceanography*, 17, 232–250. <https://doi.org/10.1016/j.mio.2016.09.005>
- Hu, C., Nelson, J. R., Johns, E., Chen, Z., Weisberg, R. H., & Muller-Karger, F. E. (2005). Mississippi River water in the Florida Stratis and in the Gulf Stream off Georgia in summer 2004. *Geophysical Research Letters*, 32, L14606. <https://doi.org/10.1029/2005GL022942>
- Le Hénaff, M., & Kourafalou, V. H. (2016). Mississippi waters reaching South Florida reefs under no flood conditions: Synthesis of observing and modeling system findings. *Ocean Dynamics*, 66, 435–459. <https://doi.org/10.1007/s10236-016-0932-4>
- Le Hénaff, M., Kourafalou, V. H., Morel, Y., & Srinivasan, A. (2012). Simulating the dynamics and intensification of cyclonic Loop Current frontal eddies in the Gulf of Mexico. *Journal of Geophysical Research*, 117, C02034. <https://doi.org/10.1029/2011JC007279>
- Mazloff, M. R., Heimbach, P., & Wunsch, C. (2010). An eddy-permitting Southern Ocean state estimate. *Journal of Physical Oceanography*, 40, 880–899. <https://doi.org/10.1175/2009JPO4236.1>
- Morey, S. L., Martin, P. J., O'Brien, J. J., Wallcraft, A. A., & Zavala-Hidalgo, J. (2003). Export pathways for river discharged fresh water in the northern Gulf of Mexico. *Journal of Geophysical Research*, 108(C10), 3303. <https://doi.org/10.1029/2002JC001674>
- Morey, S. L., Schroeder, W. W., O'Brien, J. J., & Zavala-Hidalgo, J. (2003). The annual cycle of riverine influence in the eastern Gulf of Mexico basin. *Geophysical Research Letters*, 30(16), 1867. <https://doi.org/10.1029/2003GL017348>
- Münchow, A., Melling, H., & Falkner, K. K. (2006). An observational estimate of volume and freshwater flux leaving the Arctic Ocean through Nares Strait. *Journal of Physical Oceanography*, 36(11), 2025–2041. <https://doi.org/10.1175/JPO2962.1>
- Ortner, P. B., Lee, T. N., Milne, P. J., Zika, R. G., Clarke, M. E., Podesta, G. P., et al. (1995). Mississippi River flood waters that reached the Gulf Stream. *Journal of Geophysical Research*, 100(C7), 13,595–13,601. <https://doi.org/10.1029/95JC01039>
- Otis, D. B., Le Hénaff, M., Kourafalou, V. H., McEachron, L., & Muller-Karger, F. E. (2019). Mississippi River and Campeche Bank (Gulf of Mexico) episodes of cross-shelf export of coastal waters observed with satellites. *Remote Sensing*, 11(6), 723. <https://doi.org/10.3390/rs11060723>
- Schiller, R. V., & Kourafalou, V. H. (2014). Loop Current impact on the transport of Mississippi River waters. *Journal of Coastal Research*, 30(6), 1287–1306. <https://doi.org/10.2112/JCOASTRES-D-13-00025>
- Schiller, R. V., Kourafalou, V. H., Hogan, P., & Walker, N. D. (2011). The dynamics of the Mississippi River plume: Impact of topography, wind and offshore forcing on the fate of plume waters. *Journal of Geophysical Research*, 116, C06029. <https://doi.org/10.1029/2010JC006883>
- Sturges, W., Evans, J. C., Welsh, S., & Holland, W. (1992). Separation of warm-core rings in the Gulf of Mexico. *Journal of Physical Oceanography*, 23, 250–268. [https://doi.org/10.1175/1520-0485\(1993\)023<0250:SOWCRI>2.0.CO;2](https://doi.org/10.1175/1520-0485(1993)023<0250:SOWCRI>2.0.CO;2)
- Sturges, W., & Leben, R. (2000). Frequency of ring separations from the Loop Current in the Gulf of Mexico: A revised estimate. *Journal of Physical Oceanography*, 30, 1814–1819. [https://doi.org/10.1175/1520-0485\(2000\)030<1814:FORSFT>2.0.CO;2](https://doi.org/10.1175/1520-0485(2000)030<1814:FORSFT>2.0.CO;2)
- Vazquez-Cuervo, J., Fournier, S., Dzwonkowski, B., & Reager, J. (2018). Intercomparison of in-situ and remote sensing salinity products in the Gulf of Mexico, a river-influenced system. *Remote Sensing*, 10, 1590. <https://doi.org/10.3390/rs10101590>
- Zavala-Hidalgo, J., Romero-Centeno, R., Mateos-Jasso, A., Morey, S. L., & Martinez-Lopez, B. (2014). The response of the Gulf of Mexico to wind and heat flux forcing: What has been learned in recent years? *Atmosfera*, 27(3), 317–334. [https://doi.org/10.1016/S0187-6236\(14\)71119-1](https://doi.org/10.1016/S0187-6236(14)71119-1)